DOI 10.52209/2706-977X_2025_4_110 IRSTI 55.21.99 UDC 621.1.9

Minimizing Wire Breakage in Wire Electric Discharge Machining Using Multi-Objective Artificial Bee Colony Algorithm

Pawar P. J.[1*], Dalavi A. M.[2], Thorve K. M.[1]
[1]K. K. Wagh Institute of Engineering Education and Research, Nashik, Maharashtra, India
[2]Symbiosis Institute of Technology, Pune, Maharashtra, India
[*]corresponding author

Abstract. Wire breakage in wire electric discharge machining (WEDM) is a serious issue causing in-between stoppage resulting into time loss, wastage of wire, and excessive energy utilization. Hence to achieve higher machining productivity of WEDM process, it is necessary to prevent wire breakage and also to improve material removal rates. Multi-objective optimization for maximizing material removal rate (MRR) and minimizing wire breakage in WEDM process is therefore presented in this work. A novel approach of maximizing tension sustained by the used wire for minimizing wire breakage is presented through an industrial case study. The effect of independent variables such as pulse on time, pulse off time, peak voltage, dielectric fluid pressure, wire feed rate, machine speed, and cutting speed override on dependent variables, wire breakage frequency and material removal rate is studied to formulate the optimization model based on response surface modeling. Multi-objective version of artificial bee colony algorithm is used for optimization. The set of Pareto optimal solutions obtained by this proposed approach provides a ready reference to select most appropriate parameter setting on the machine.

Keywords: WIRE electric discharge machining, wire breakage, material removal rate, multi-objective artificial bee colony algorithm

Introduction

Wire electric discharge machining (WEDM) is an important process, specially used to make complex and intricate shaped components from difficult to machine materials. The wire breakage is one of the major issues frequently encountered while wire electric discharge machining of hard materials like EN19 commonly used for defense applications. While machining if wire breaks, it will stop the operation in serious situation. After breakage all the operation settings has to recover and broken wire has to replace. It is difficult to restart the machining operation from the same work-piece and tool alignment settings. Thus this replacement increases the machining time. Wire breakage also produces a permanent surface damaged on the component surface and also decreases accuracy of the process. This will greatly hamper the machining performance and productivity of WEDM.

The wire breakage in WEDM occurs due to several causes including the thermal loading, high wire tension due to intricate and complex shape of components, impact of electric discharge and large vibrations of wire etc. The machining parameters that affects MRR and wire breakage includes pulse on time, pulse off time, peak voltage, wire feed, flushing pressure, machine speed and cutting speed etc. For the high electric discharge higher pulse on time is required to select which causes the short circuit and wire breakage. On the other hand, higher value of pulse off time reduces the risk of wire breakage but reduces MPR. The peak voltage directly affects the wire breakage. Due to the higher value of peak voltage, heat energy increases which leads to melting and vaporization of wire. The selection of proper wire feed rate results into higher material removal rate, less wire breakage and better surface finish. Flushing pressure refers to the pressure of flushing fluid used to remove the molten slug. The high flushing pressure causes the wire deflection and vibrations, but it is also necessary for better cutting performance. Material removal rate is equally important to achieve higher machining productivity and cost effective utilization of machine. While selecting appropriate parameters for minimum frequency of wire breakage care has to be taken that material removal rate should not be hampered. As these two objectives i.e. minimization of frequency of wire breakage and maximization of material removal rate are conflicting in nature, selection of appropriate process parameters is a challenging task.

Several attempts are made by the researchers for the investigation of wire breakage in WEDM. Kinoshita et al. [1] experimentally studied the conditions of wire breakage and noticed its various reasons and presented a control strategy for prevention of wire breakage by monitoring the pulse frequency. Rajurkar et al. [2] presented the relationship between sparking frequency and wire breakage in WEDM and noticed that wire rupture occurs at high sparking frequency. Based on this a control strategy was suggested to maintain sparking frequency to constant level by on line monitoring. Yan and Liao [3] developed a fuzzy logic based adaptive control optimization system to investigate various performance measures such as material removal rate, surface roughness, and wire breakage. Liao et al. [4] identified two causes of wire rupture namely excess of sparks and sudden rise of sparking frequency. Yan and Liao [5] developed a multi variable three region fuzzy controller for online monitoring of abnormal sparks and sparking frequency to prevent the wire breakage. Luo [6] presented the effect of various WEDM parameters on wire failure and mechanical strength of wire electrode. The study revealed that wire yielding and fracture are the main causes of wire rupture. Inadequate flushing causes the wire temperature increase which also leads to wire failure and the spark pressure directly affects the bow error which also has importance in wire rupture. Guo et al. [7] through simulation modeling of wire vibration observed that under the optimum conditions of discharge energy, discharge frequency, wire tension, and wire span the wire breakage can be minimized. Saha et al. [8]

developed a finite element model for the heat distribution of wire and predicted that the non- uniform heat generated in wire causes the wire breakage; also an optimization process was developed for minimizing the temperature of wire to reduce thermal strain. Cabanes et al. [9] developed a new wire breakage monitoring and diagnosing system by analyzing experimental data to predict the conditions for the wire breakage such as discharge energy, peak current, and ignition delay time. Kumar et al. [10] analyzed the wire electrode surface after the machining of titanium using Energy Dispersive X-ray and revealed that the wire breakage is due to large temperature value during machining of titanium. Gupta et al. [11] investigated the effect of pulse on time, pulse off time, voltage and wire feed rate for minimum surface roughness, wire breakage and maximum material removal rate. Okada et al. [12] attempted to correlate the kerf length and nozzle jet flushing with wire deflection and breakage. Habib and Okada [13] revealed that unstable wire behavior and large vibrations of wire electrode has serious effect on wire breakage, reduction in accuracy and low surface finish. Kumar et al. [14] discussed a detail review of researches and their findings about the major problems that frequently encountered in application of WEDM. Das and Joshi [15] presented an approach to estimate the wire safety index based on thermal residual stresses that generate on the wire electrode by using a finite element method based model. Abhilash and Chakrdhar [16] developed an approach to correlate the mean gap voltage variation and wire breakage occurrences during the wire EDM of Inconel material. Earlier researchers also attempted multi-objective optimization of WEDM for minimization of wire breakage and material removal rate using priori approach [17], Taguchi Method [18], Response Surface Methodology [19, 20], Particle swarm optimization [21], Teaching Learning Based Optimization [22, 23], Adaptive Nuro-fuzzy Interface System [24], Neural network [25], Support vector machine [26] etc.

For multi-objective optimization, researchers are mainly employing two approaches - priori approach and posteriori approach. In priori approach, weights are assigned to the different objectives before optimizing. However, if the process engineer does not have compressive knowledge of the process, there is always a chance of selecting inappropriate weights leading to ineffective solution. Hence, for multi-objective optimization, posteriori approach is preferred which provides non-dominated set of optimum solutions. The decision maker is free to choose any solution from this set of optimum solutions. Artificial bee colony algorithm developed by Karaboga and Basturk [27] has been proved to be one of the most powerful and robust algorithms for optimization of several real life applications. In this work an attempt is made to apply multi-objective version of artificial bee colony algorithm proposed by Pawar et al. [28] which is based on the concept of non-dominated sorting [29] as discussed in the next section.

1. Multi-Objective Artificial Bee Colony Algorithm

The artificial bee colony algorithm [27] is inspired by the intelligent behavior of honey bee swarms to search a food source rich in nectar and close to their hive. Just like natural honeybee system, this algorithm models also consist of three groups of bees: onlooker bees, employed bees, and scout bees. Employed bees exploit a source of food and also share the information about this food source to onlooker bees, onlooker bees will use the information shared by employed bees to evaluate quality of food source, scout bees discover all food source positions randomly. To extend the application of ABC algorithm for multi-objective optimization with posteriori approach, concept of non-dominated sorting [29] is incorporated in this work. Once the initial population and fitness function is evaluated, the non-dominated sorting of solutions is carried out to rank the solutions till all the solutions got non-dominated status. Based on the rank of the solution the shared fitness values is calculated. The probability to which the onlooker bee is assigned to employed bee is then calculated based on this shared fitness and not based on actual fitness. The rest of the procedure is same as that of artificial bee colony algorithm.

2. Application Example

An application example considered in this work is a special tool for defense application made of EN19 steel material. The details of experimental set up used for data collection are given below:

- Machine type = ULTIMA 1S/2S (Wire cut WEDM submerged type);
- Pulse Generator = ELPULS 55S SERIES;
- Make= Electronica Machine tools;
- Wire material = Brass diffusion coated;
- Wire diameter = 0.25 mm;
- Wire composition = Cu 65% and Zn 35%;
- Wire strength = 400 N/mm^2;
- Wire tension = 19.63 Newton;
- Dielectric = distilled water (HCl and Carbide soda);
- Range of dielectric temperature = 20°C to 240°C.

Due to chromium, molybdenum and manganese in EN 19 steel, it has high abrasion and impact resistance, high fatigue strength, high toughness and torsional strength. Because of the high hardness and high strength of EN 19 steel it finds greater utility in the defense applications. However, due to these distinct properties of EN 19 material, the conventional machining processes are not suitable for machining of this material. In nontraditional machining processes, the wire electric discharge machining process find suitable for machining of EN 19 material. The wire electric discharge machining is mostly used in applications of making complex and intricate shapes (which are either two or three dimensional) from difficult to machine materials by means of erosion. However, there are certain problems in wire electric discharge machining of EN 19 material. These include the low material removal rate, high wire electrode wear rate, and poor surface finish. During wire electric discharge machining of EN 19 material, large size craters are produce on the wire electrode. These craters increase the chance of wire breakage and ultimately lead to lowering the surface finish and dimensional accuracy of work-piece. The wire electrode breakage during wire electric discharge machining results in harmful and highly undesirable distortions of surface of machined component as well as it decreases the accuracy of machining. It has been experimentally found that the wire electrode breakage is increases with increase in pulse duration and open circuit voltage and it is decreases with decrease in wire speed. As the higher pulse duration, peak voltage and wire speed etc. are essential for better material removal rate value but these leads to greater wire wear rate. The schematic sketch of WEDM process showing wire feed mechanism is shown in Fig. 1.

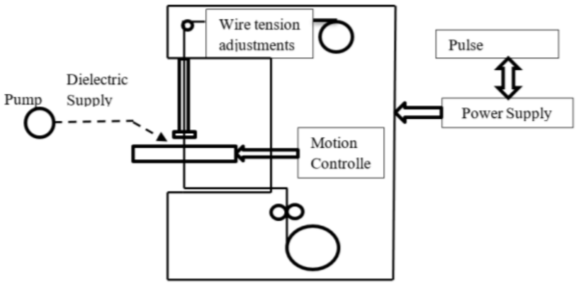

Fig. 1. - Schematic sketch of WEDM process showing wire feed mechanism

Keeping in view the above-mentioned aspects of product manufacturing, the two objectives considered are (i) Minimization of frequency of wire breakage (by ensuring that tension sustained by the used wire, T_{uw} is maximum) (ii) Maximization of material removal rate (R). To minimize the frequency of wire breakage, the parameters should be so selected that the minimum tensile stress should be induced in the wire. For this, the tension sustained by the used wire before breakage is measured. It is obvious that for the parameter setting for which the tension withstand by the used wire is maximum, the risk of the wire breakage is also minimum. The important process variables identified affecting the above mentioned responses are: pulse on time (T_{on}), Pulse off time (T_{off}), Peak voltage (V_p), dielectric fluid pressure (P_w), Wire feed rate (f), Machine speed (V_m), and Cutting speed override (O). Operating ranges of these process variables and their coded levels are presented in Table 1.

Table 1. Process variables and their coded values

Parameters	**Coded levels**				
	-α	**-1**	**0**	**1**	**α**
T_{on} (μsec)	103	105	107	109	111
T_{off} (μsec)	23	30	37	44	51
V_p (Volts)	10	11	12	13	14
P_w (Kgf/cm^2)	7	11	15	19	23
f (mm/min)	2	3	4	5	6
V_m (RPM)	75	100	125	150	175
O (%)	15	20	25	30	35

A response surface model is obtained by conducting 149 experiments as the number of independent variables are 7. The details of these 149 experiments are provided in Appendix-I. A second-order polynomial response is fitted into the following equation to study the effect of independent variables on dependent variables as given by Eq. (1) and Eq. (2) provided in appendix 1.

To test whether the data are well fitted in model or not, the calculated r^2value of the regression analysis for material removal rate (R) and tension withstand by the used wire (T_{uw}) are obtained as 0.97 and 0.87 respectively. The high r^2 values obtained for both the responses clearly indicate that the regression models developed in this work fit the data well. The next section describes the application of non-dominated sorting based artificial bee colony algorithm for parameter optimization of wire electric discharge machining.

3. Multi-Objective Optimization using Non-Dominated Sorting Based Artificial Bee Colony Algorithm

To demonstrate and validate the proposed approach, following multi-objective optimization model is formulated:

Objective 1: Maximization of material removal rate (R) as given by Eq. (1)

Objective 2: Maximization of tension that the used wire can withstand without breakage (T_{uw}) as given by Eq. (2).

Although the population size is of 50 is considered in this work, only first five solutions are considered for demonstration. The proposed approach is demonstrated through following steps.

Step 1: Parameters selection:

- Number of employed bees (=Number of food sources): 20
- Number of onlooker bees: 50
- Number of scout bees: 1

Step 2: Calculate the nectar amount for each food source

The nectar amount of each food source is obtained by evaluating the objective function values as shown in Table 2.

Table 2. Nectar amount (in terms of R and T_{uw}) for each food source

Solution No.	T_{on} (μsec)	T_{off} (μsec)	V_p (Volts)	P_w (kgf/cm^2)	f (mm/min)	V_m (RPM)	O (%)	R (mm^3/min)	T_{uw} (N)
1	104.6	47.1	11.3	11.8	3.4	80.4	35.0	0.93	3.25
2	110.6	23.0	12.6	14.7	5.2	137.4	19.8	0.87	3.30
3	108.5	46.2	14.0	12.1	3.8	174.9	16.2	1.09	2.65
4	105.9	49.7	11.4	12.0	4.5	162.6	31.1	0.91	3.08
5	110.8	35.1	11.0	11.1	3.1	140.0	16.7	0.87	3.43

Step 3: Non-dominated sorting of solutions

The solutions are ranked based on non-dominated sorting as shown in Table 3.

Table 3. Rank assigned to each solution

Solution No.	R (mm^3/min)	T_{uw} (N)	Rank
1	0.93	3.25	3
2	0.87	3.30	2
3	1.09	2.65	2
4	0.91	3.08	4
5	0.87	3.43	2

Step 4: Determine normalized Euclidean distance of each solution

Table 4 shows normalized Euclidean distance of each solution from every other solution is calculated using Eq. (3).

$$d_{ij} = \sqrt{\sum\left(\frac{x_s^i - x_s^j}{x_s^{max} - x_s^{min}}\right)^2} \qquad (3)$$

Table 4. Normalized Euclidean distance of each solution

Solutions	1	2	3	4	5
1	0.00	1.60	1.58	0.91	1.41
2	1.60	0.00	1.10	1.33	0.84
3	1.58	1.10	0.00	1.06	0.98
4	0.91	1.33	1.06	0.00	1.16
5	1.41	0.84	0.98	1.16	0.00

Step 5: Determine niche count of the solution

A niche count (nc_i) provides an estimate of the extent of crowding near a solution and is calculated using the equation:

$$nc_i = \sum sh(d_{ij}) \qquad (4)$$

where, Sh(d_{ij}) is the sharing function values of all the first front solutions as given by equation:

$$Sh(d_{ij}) = \left\{1 - \left(\frac{d_{ij}}{\sigma_{share}}\right)^2\right\} \quad if \ d_{ij} < \sigma_{share} \qquad (5)$$

$= 0$ otherwise

where, σ_{share} is the maximum distance allowed between any two solutions to become members of a niche. The σ_{share} value in this equation is to be chosen appropriately. The sharing function values shown in Table 5 are obtained by using Eq. (5).

Table 5. Sharing function values of each solution

Solutions	Sharing function values				
	1	2	3	4	5
1	1.00	0.00	0.00	0.17	0.00
2	0.00	1.00	0.00	0.00	0.29
3	0.00	0.00	1.00	0.00	0.04
4	0.17	0.00	0.00	1.00	0.00
5	0.00	0.29	0.04	0.00	1.00

Niche count for first 5 solutions is then obtained using Eq. (4) as given in Table 6 below.

Table 6. Niche count of each solution

Solution No.	1	2	3	4	5
Niche count (N_c)	2.22	2.62	1.79	2.74	2.20

Step 6: Determine the shared fitness values of the solutions:
Considering the dummy fitness value for rank 1 solutions as 50, the shared fitness values for 5 sample solutions are obtained using Eq. 6) and are presented in Table 7.
Shared fitness (F_i) = Dummy fitness (f) / nc_i (6)

Table 7. Shared fitness values

Solution No.	1	2	3	4	5
Shared Fitness	1.26	5.25	7.66	0.34	6.24

Step 7: Determine the probabilities based on the shared fitness values evaluated in step 6:
The probability (P_i) with which the onlooker bee is assigned to employed bee is obtained based on the shared fitness is obtained using Eq. (7) as shown in Table 8:

$$P_i = \frac{\sum_{k=1}^{R} (1/f_k)^{-1}}{f_i} \tag{7}$$

Table 8. Probabilities of assigning onlooker bees to employed bees

Solution No.	1	2	3	4	5
P_i	0.008	0.032	0.047	0.002	0.038

Step 8: Calculate the number of onlooker bees, which will be sent to food sources
The number of onlooker bees sent to an employed bee (N) shown in Table 10 are obtained using Eq. (8) below:

$$N = P_i \times m. \tag{8}$$

Where, 'm' is the total number of onlooker bees.

Table 9. Number of onlooker bees assigned to employed bees

Solution No.	1	2	3	4	5
N	0	2	2	0	2

Step 9: Determine new position of each onlooker bee
Each food source position is updated 'N' times using the Eq. (9):

$$x_i' = x_i \pm (x_j - x_k) \tag{9}$$

Where, x_i' is updated food source position, x_i is current food source position, x_j and x_k are randomly chosen food source position from current population. Each food source is then updated if better position is obtained by onlooker assigned to that food source.

The positions of these onlooker bees are obtained as mentioned in Table 10.

Table 10. Positions of onlooker bees

Solution No.	Position of onlooker bee 1	R (mm^3/min)	T_{uw} (N)	Position of onlooker bee 2	R (mm^3/min)	T_{uw} (N)
2	(110.2, 23.1, 12.4, 13.6, 5.3, 141.7, 21.0)	0.83	3.34	(111.0, 23.7, 12.4, 14.1, 5.3, 137.7, 19.0)	0.89	3.31
3	(108.4, 48.3, 14.0, 11.3, 3.6, 175.0, 17.1)	1.04	2.63	(108.9, 44.8, 14.0, 12.2, 4.2, 175.0, 15.8)	1.11	2.65
5	(110.9, 34.3, 10.7, 12.4, 2.8, 133.8,17.4)	0.81	3.52	(110.8, 35.0, 11.2, 11.7, 3.4, 146.3, 17.4)	0.90	3.32

The positions of onlooker bees for each food source are then compared with the position of the employed bee assigned to that food source. The priori approach is used to for comparing the new solution with the old one, so as to make the decision whether to replace the old solution with new solution or not. For evaluating combined objective function equal weights of both objectives are considered. The combined objective function (to be minimized) is then evaluated as:

$$Z = -\frac{R}{R^*} - \frac{T_{uw}}{T_{uw}^*} \qquad (10)$$

where R^* and T_{uw}^* are threshold values of material removal rate and tension sustained by used wire respectively.

The values of combined objective functions for employed and onlooker bees using Eq. (10) are shown in Table 11. In MO-ABC approach, the non-dominated sorting is performed on original population of solutions. Hence, the rank 1 solutions will be given a chance multiple times to generate better solution, as the number of bees assigned to a solution is based on shared fitness value. Thus it is ensured that diversity is maintained for Pareto optimality. However, the priori approach is used just to get a reference value for choosing the best among the newly generated solution. However, anyway the so chosen solutions will have to undergo non-dominated sorting in the next generation. The equal weights for the objectives are used for unbiased selection.

Table 11. Combined objective functions for employed and onlooker bees

Solution No.	'Z' for employed bee	'Z' for onlooker bee 1	'Z' for onlooker bee 2
2	-1.29	-1.27	-1.30
3	-1.29	-1.26	-1.31
5	-1.314	-1.29	-1.31

It is observed from the above Table that combined objective function values of onlooker bee 2 and 3 are better than those of corresponding employed bee, hence the solution 2 and solution 3 are updated. For solution 5, combined objective function value of employed bee is better than both those of both the onlooker bees hence the position of the employed bee is retained. Table 12 shows the new set of first five solutions.

Table 12. Set of updated Solutions

Solution No.	Updated employed bee position	Z
1	(104.6, 47.1, 11.3, 11.8, 3.4, 80.4, 35)	-1.315
2	(111.0, 23.7, 12.4, 14.1, 5.3, 137.7, 19.0)	-1.303
3	(108.9, 44.8, 14, 12.2,4.2, 175.0, 15.8)	-1.309
4	(105.9, 49.7, 11.4, 12.0,4.5,162.6, 31.1)	-1.266
5	(110.8, 35.1,11.0,11.1,3.1,140.0,16.7)	-1.314

This process maintains elitism as best among new solutions is compared with old solution and the one which is superior gets selected.

Step 10: Evaluate the best solution

The global best of the honeybee swarm is (107.1, 32.4, 11.8, 18.9, 5.6, 75, 15) with value of R and T_{uw} as 1.05 mm^3/min and 3.47 N respectively.

Step 11: Update the scout bee

Since number of scout bee is one, a random solution is generated as (104.2, 33.3, 12.6, 23.0, 3.1, 148.7, 22.4) with Z = -1.163. The worst of the updated solution is (106.2, 50.5, 11.7, 12.5, 4.6, 165.8, 30.9) with Z = -1.266. Since, the worst solution is better than the randomly generated (scout) solution, the worst solution will not be replaced by scout solution.

Step 12: Obtain the set of Pareto-optimal solution

The steps 2-11 are iterated for 140 generations to obtain the set of Pareto optimal solution as shown in Table 13. Although 20 initial solutions were considered, the algorithm is able to maintain the diversity in the population resulting into 13 Pareto optimal solutions.

Table 13. Set of Pareto optimal solutions

S. N.	T_{on} (μsec)	T_{off} (μsec)	V_p (Volts)	P_w (kgf/cm^2)	f (mm/min)	V_m (RPM)	O (%)	R (mm^3/min)	T_{uw}(N)
1	111.0	51.0	14.0	22.9	4.6	175.0	35.0	1.34	2.29
2	111.0	51.0	12.0	22.2	5.2	89.8	35.0	1.30	2.58
3	111.0	51.0	11.4	23.0	4.9	125.6	35.0	1.25	2.74
4	110.4	46.9	10.5	18.6	4.9	164.4	15.0	1.10	3.33
5	109.6	50.9	10.7	16.5	5.2	75.0	15.0	1.05	3.62
6	108.7	51.0	10.4	17.4	5.3	75.0	15.0	1.02	3.73
7	110.9	51.0	10.0	18.0	5.2	87.3	15.0	1.00	3.77
8	110.0	51.0	10.3	15.3	5.3	75.0	15.0	1.00	3.81
9	111.0	51.0	10.0	16.2	5.1	75.0	15.0	0.98	3.85
10	111.0	50.9	10.0	15.3	5.3	75.0	15.0	0.97	3.88
11	107.1	51.0	10.4	15.0	5.2	75.0	15.0	0.96	3.90
12	109.3	51.0	10.0	12.9	5.3	75.0	15.0	0.91	4.07
13	106.9	51.0	10.0	13.7	5.5	75.0	15.0	0.88	4.16

This set of Pareto optimal solution can be used as ready reference by the process engineers to select the most appropriate solution as per his/her requirement. The Pareto-front is shown in Fig. 2.

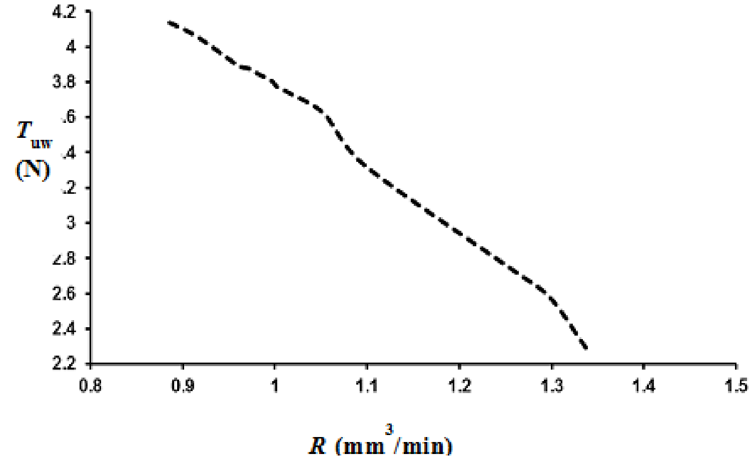

Fig. 2. - Pareto front

The effect of each process variable (while keeping other variables at their optimum level) on material removal rate and frequency of wire breakage is presented through Figures 4 to 10.

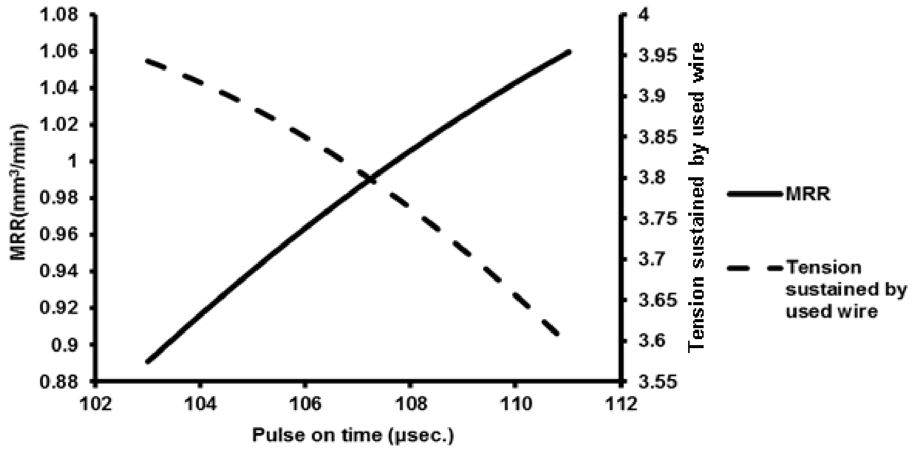

Fig. 3. - Effect of pulse-on time on objective functions

As shown in Fig. 3, material removal rate increases with increase in pulse on time as, with increase in pulse on time electric discharge rate increases. However, increased electric discharge rate also increases chance of wire breakage as indicated by reduction in tension sustained by used wire. Fig. 4 shows that the material removal rate increases with increase in pulse off time as, with increase in pulse off time better flushing of debris take place from the inter-electrode gap, resulting in increase in MRR. However, with increase in pulse off time the tension sustained by used wire decreases.

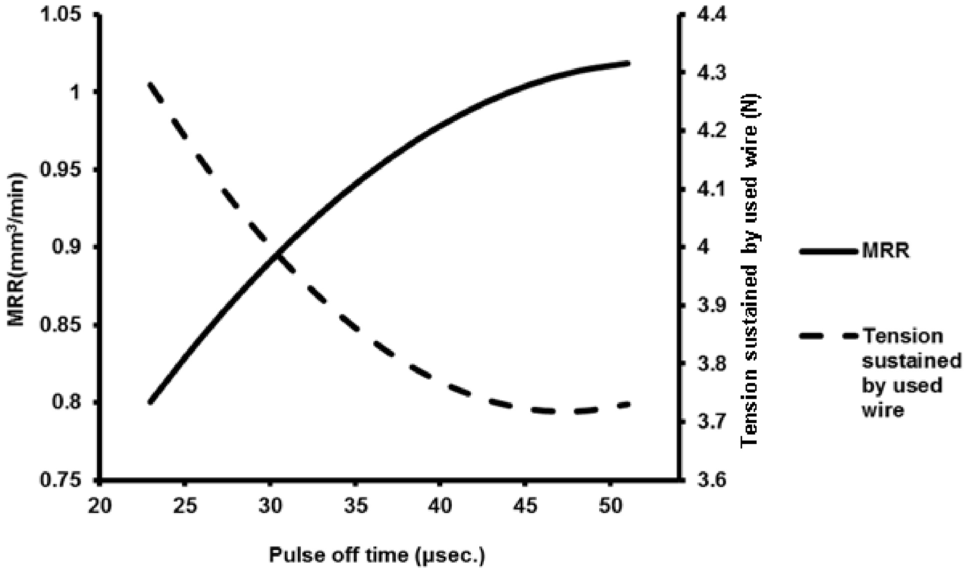

Fig. 4. - Effect of pulse-off time on objective functions

As shown in Fig.5, the peak voltage has significant effect on both the objectives. Material removal rate initially increases with increase in peak voltage up to 13 volts and then start decreasing. Also, at higher peak voltage large amount of heat is generated which results into overheating of wire electrode. Hence with increase in peak voltage the tension sustained by used wire the decreases indicating more chances of wire breakage.

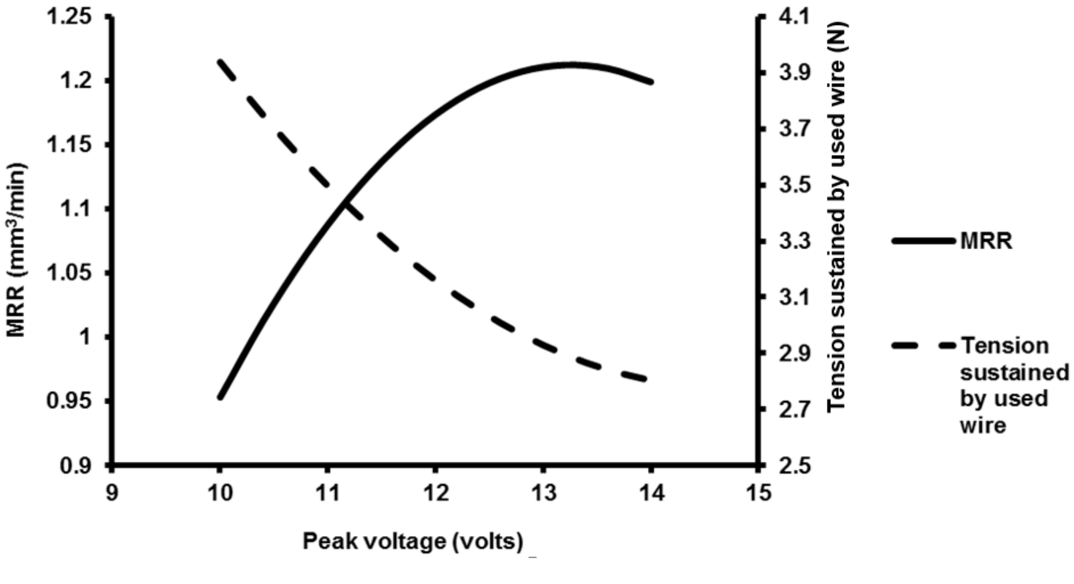

Fig. 5.- Effect of peak voltage on objective functions

The effect of dielectric fluid pressure on material removal rate and tension sustained by used wire is shown in Fig. 7. Increasing dielectric fluid pressure increases flushing rate which results into higher material removal rate. However, higher dielectric fluid pressure causes more force acting on wire electrode which increases chances of wire breakage. The effect of wire feed rate on material removal rate and tension sustained by used wire is shown in Fig. 7. Increasing wire feed rate increases Material removal rate. The tension sustained by used wire also increases initially (up to wire feed rate of 4.5 mm/min) and then decreases with increase in wire feed rate. This is due to the fact that above certain value of feed rate, bowing effect on wire electrode increases critically resulting into higher chances of wire breakage.

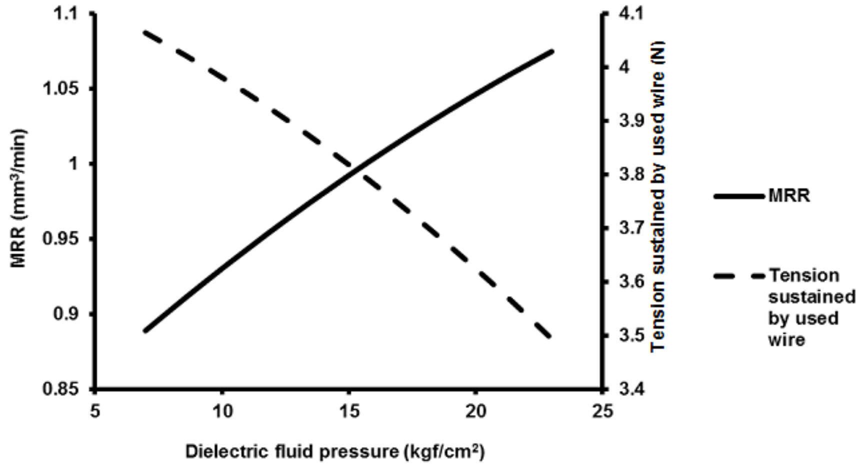

Fig. 6. - Effect of dielectric fluid pressure on objective functions

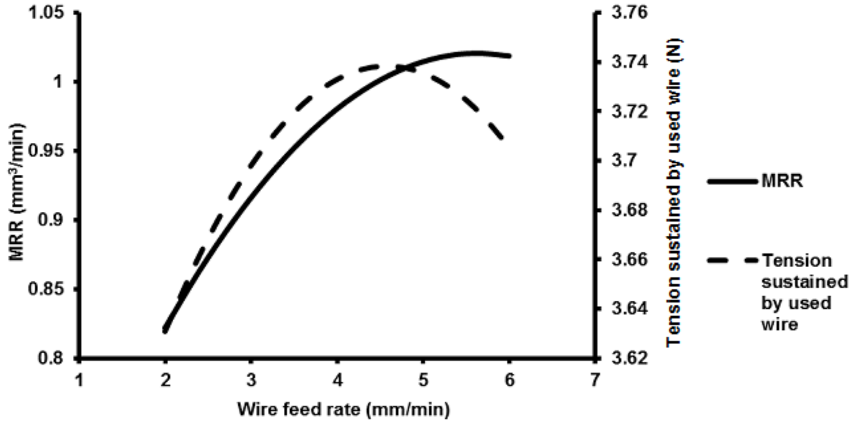

Fig. 7. - Effect of wire feed rate on objective functions

The effect of machine speed on material removal rate and tension sustained by used wire is shown in Fig. 8. The material removal rate increases with increase in machine speed. However, the tension sustaining capacity of used wire decreases with increase in machine speed. The effect of cutting speed override on material removal rate and tension sustained by used wire is shown in Fig. 9. The material removal rate initially decreases with increase in cutting speed override and becomes minimum at 25% override, after that it increases with further increase in cutting speed override. It can also be seen that the tension sustaining capacity of used wire decreases with increase in machine speed.

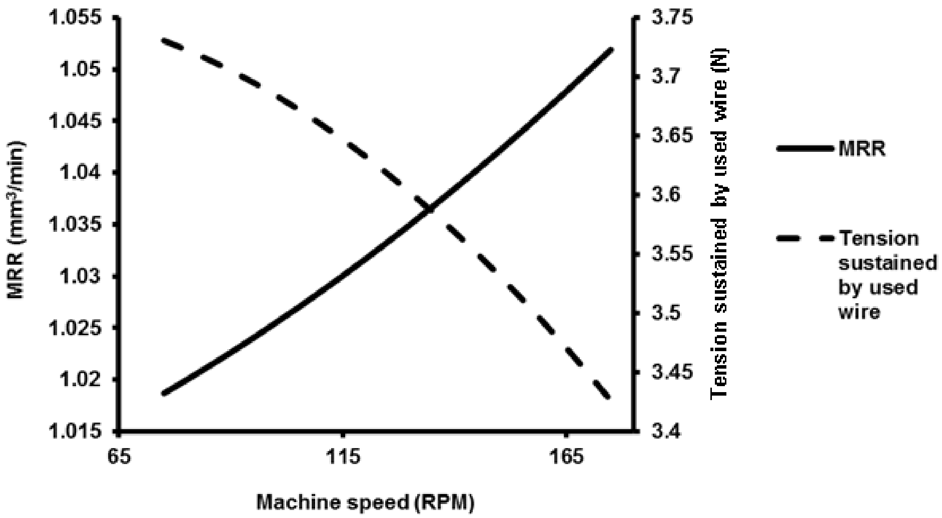

Fig. 8. - Effect of machine speed on objective functions

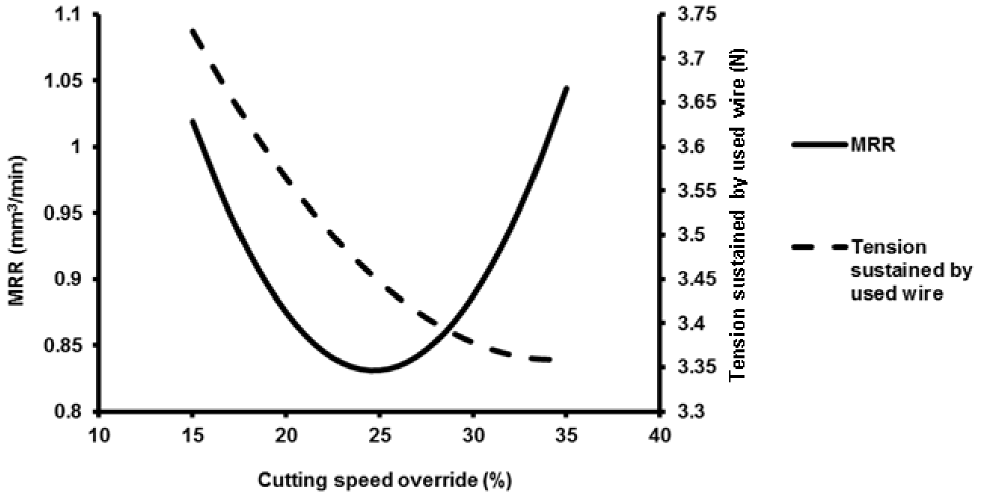

Fig. 9. - Effect of cutting speed override on objective functions

Although the parameters ranges available on machine are very wide, this study reveals that parameter values in some specific ranges only are effective to achieve better process performance of wire electric discharge machining process with respect to material removal rate and frequency of wire breakage. The most effective ranges of process variables to ensure best performance with respect to both objectives considered in this work are provided by value path plot as shown in Fig. 10.

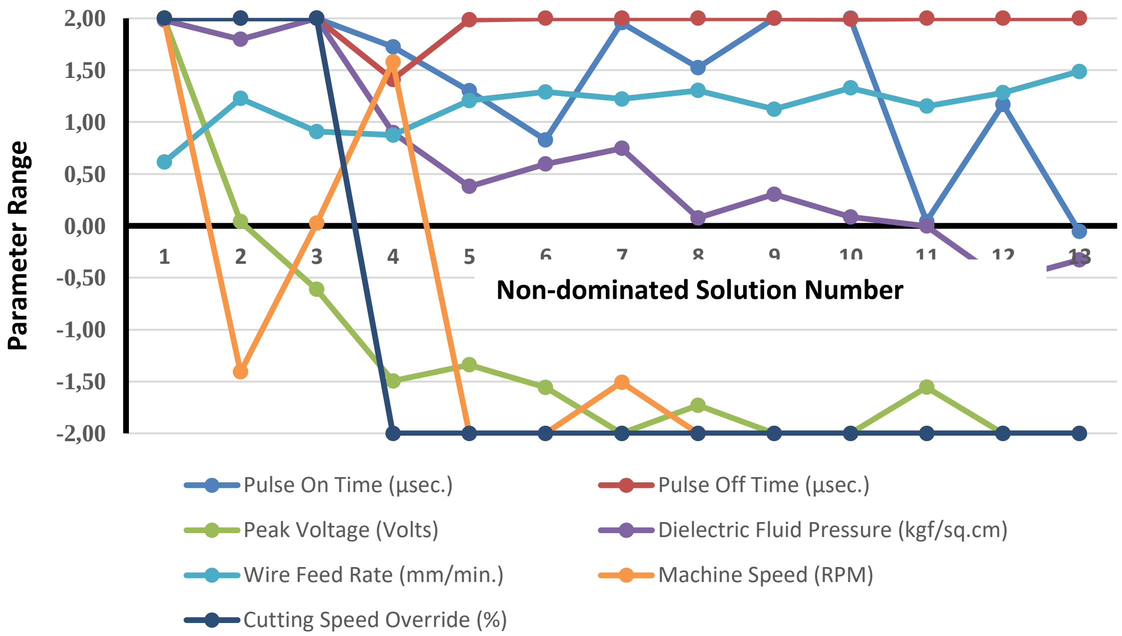

Fig. 10. - Value path plot

Conclusions

Wire breakage and low material removal rate are serious issues in wire electric discharge machining especially for machining of hard to cut materials with complex profiles. In this work, multi-objective version of artificial bee colony algorithm based on the concept of non-dominated sorting is proposed to deal with issues. The two objectives considered are: minimizing frequency of wire breakage and maximization of material removal rate. A concept of maximizing tension sustained by used wire is applied to ensure minimum frequency of wire breakage. A set of 13 non-dominated solutions is obtained using proposed multi-objection optimization approach. This provides ready reference to process engineers to set best operating parameters on machines as per his/her requirements. Value path plot reveals that from wire breakage and MRR point of view most effective ranges of process parameters are: pulse on time: 107-111 µsec, pulse off time: 47-51 µsec, peak voltage: 10-10.8 Volts, dielectric fluid pressure: 13-19 kg/cm^2, wire feed rate: 4.5-5.5 mm/min, machine Speed:

5-175 rpm and cutting speed override: 15-35 %. Combined objective function values for set of non-dominated solutions obtained by using proposed multi-objective ABC algorithm shows an average improvement of about 17.9% over those obtained by initial data set obtained experimentally. This clearly indicate the effectiveness of the proposed approach of maximizing the tension sustained by used wire to minimize the wire breakage in wire electric discharge machining of hard materials like EN19.

Declaration of Competing Interest. The authors declare that they have no known competing of interest.

References

[1] Kinoshita N., Fukui M., Gamo G. Control of wire – EDM preventing electrode from breaking //CIRP Ann Manuf Technol., 1982, Vol. 31, P. 111 – 114.
[2] Rajurkar K. P., Wang W. M., Lindsay R.P. On-line monitor & control for wire breakage in WEDM //CIRP Ann Manuf Technol., 1991, Vol. 40, P. 219 – 222.
[3] Yan M. T., Liao Y. S. Monitoring & self-learning fuzzy control for wire rupture prevention in wire electrical discharge machining //Int. J. Mach. Tools Manuf., 1996, Vol. 36, P. 339 – 353.
[4] Liao Y. S., Chu Y. Y., Yank M. T. Study of wire breaking process & monitoring of WEDM // Int. J. Mach. Tools Manuf., 1997, Vol. 37, P. 555 – 567.
[5] Yan M. T., Liao Y. S. Adaptive control of the WEDM process using the fuzzy control strategy //Journal of Manufacturing Systems, 1998, Vol. 17, P. 263 – 274.
[6] Luo Y. F. Rupture failure & mechanical strength of the electrode wire used in wire EDM //J. Mater. Process. Technol., 1999, Vol. 94, P. 208 – 215.
[7] Guo Z. N., Yue T. M., Lee T. C., Lau W. S. Computer simulation & characteristic analysis of electrode fluctuation in wire electric discharge machining //J. Mater. Process. Technol., 2003, Vol.142, P. 576–581.
[8] Saha S., Pachon M., Ghoshal A., Schulz M. J. Finite element modeling & optimization to prevent wire breakage in electro-discharge machining //Mech. Res. Commun., 2004, Vol. 31, P. 451–463.
[9] Cabanes I., Portillo E., Marcos M., Sanchez J. A. On-line prevention of wire breakage in wire electro - discharge machining //Robot Comput Integr Manuf., 2008, Vol. 24, P. 287–298.
[10] Kumar A., Kumar V., Kumar J. Microstructure analysis & material transformation of pure titanium & tool wear surface after wire electric discharge machining process //Mach. Sci. Technol., 2014, Vol. 18, P. 47–77.
[11] Gupta K., Chaube S. K., Jain N. K. Exploring wire – EDM for manufacturing of high quality meso – gears //Procedia Materials Science, 2014, Vol. 5, P. 1755 – 1760.
[12] Okada A., Konishi T., Okamoto Y., Kurihara H. Wire breakage & deflection caused by nozzle jet flushing in wire EDM //CIRP Ann Manuf Technol., 2015, Vol. 64, P. 233 – 236.
[13] Habib S., Okada A. Study on the movement of wire electrode during fine wire electrical discharge machining process //J. Mater. Process. Technol., 2016, Vol. 227, P.147–152.
[14] Kumar S., Goyal K. K., Kumar R. Research trends in Wire electrical discharge machining (WEDM): A Review // Int. J. Technol. Res. Eng., 2015,Vol. 2, P. 1164 – 1171.
[15] Das S., Joshi S. N. Estimation of wire strength based on residual stresses induced during wire electric discharge machining // J. Manuf. Process., 2020, Vol. 53, P. 406-419.
[16] Abhilash P.M., Chakradhar D. ANFIS modelling of mean gap voltage variation to predict wire breakages during wire EDM of Inconel 718 //CIRP J Manuf Sci Technol., 2000, Vol. 31, P. 153-164.
[17] Ramakrishnan R., Karunamoorthy L. Multi response optimization of wire EDM operations using robust design of experiments //Int. J. Adv. Manuf. Technol., 2006, Vol. 29, P.105–112.
[18] Nourbakhsh F., Rajurkar K. P., Malshe A. P., Cao J. Wire electro-discharge machining of titanium alloy //Procedia CIRP, 2014,Vol. 5, P. 13 – 18.
[19] Mandal A., Dixit A. R., Das A. K., Mandal N. Modeling & optimization of machining Nimonic C-263 super alloy using multi-cut strategy in WEDM //Mater. Manuf. Process., 2015, Vol. 31, P. 860 – 868.
[20] Habib S. Optimization of machining parameters & wire vibration in wire electrical discharge machining process //Mech. Adv. Mater. Struct., 2017, Vol. 3, paper 3.
[21] Nain S. S., Dixit G., Kumar S. Performance evaluation of the WEDM process of aeronautics super alloy //Mater. Manuf. Process., 2018, Vol. 33, P.1793-1808
[22] Devarasiddappa D., Chandrasekaran M. Experimental investigation & optimization of sustainable performance measures during wire-cut EDM of Ti-6Al-4V alloy employing preference-based TLBO algorithm //Mater. Manuf. Process., 2020, Vol. 35, P. 1204-1213.
[23] Shandilya P., Rouniyar A. K., Saikiran D. Multi-objective parametric optimization on machining of Inconel-825 using wire electrical discharge machining //J. Mech. Eng. Sci., 2020, Vol. 234, P. 4056-4068
[24] Phate M., Bendale A., Toney S., Phate V. Prediction & optimization of tool wear rate during electric discharge machining of Al/Cu/Ni alloy using adaptive neuro-fuzzy inference system // Heliyon, 2020, Vol. 6, e5308
[25] Chou P-H, Hwang Y-R, Yan B-H The study of machine learning for wire rupture prediction in WEDM // Int. J. Adv. Manuf. Technol., 2022, Vol. 119, P. 1301-1311.
[26] Goswami K., Samuel G. L. Support vector machine regression for predicting dimensional features of die-sinking electrical discharge machined components //Procedia CIRP, 2021, Vol. 99, P. 508–513.
[27] Karaboga D., Basturk B. On the performance of artificial bee colony (ABC) algorithm // Applied Soft Computing, 2008, Vol. 8, P. 687-697.
[28] Pawar P. J., Vidhate U. S., Khalkar M. Y. Improving the quality characteristics of abrasive water jet machining of marble material using multi-objective artificial bee colony algorithm // J Comput Des Eng., 2018, Vol. 5, P. 319-328.
[29] Deb K. Multi-objective optimization using Evolutionary Algorithms. - Wiley India Pvt. Ltd., India, 2005.

Appendix 1

$$R=0.8486+0.0477.x_1+0.058.x_2+0.066.x_3+0.043.x_4+0.033.x_5+0.0088.x_6+0.0044.x_7\,\_0.0026.x_1^2-0.0119.x_2^2-0.0244.x_3^2-0.0026.x_4^2-0.015.x_5^2+0.0005.x_6^2+0.050.x_7^2-0.0015.x_1.x_2-0.0015.x_1.x_3+0.0015.x_1.x_4-0.00078.x_1.x_5+0.00078.x_1.x_6+0.00156.x_1.x_7-0.00156.x_2.x_3+0.00078.x_2.x_4-0.0015.x_2.x_5+0.x_2.x_6+0.00156.x_2.x_7+0.00156.x_3.x_4-0.00078.x_3.x_5-0.00078.x_3.x_6+0.00078.x_3.x_7+0.x_4.x_5+0.x_4.x_6-0.0015.x_4.x_7-0.0054.x_5.x_6-0.0039.x_5.x_6-0.0023.x_6.x_7 \quad (1)$$

$$T_{\mathrm{uw}}=3.079-0.0845.x_1-0.1514.x_2-0.2536.x_3-0.086.x_4+0.0463.x_5-0.04485.x_6-0.0720.x_7-0.0099.x_1^2+0.0463.x_2^2+0.0525.x_3^2-0.0099.x_4^2-0.01617.\ x_5^2-0.0099.x_6^2+0.0244.x_7^2+0.0093.x_1.x_2-0.00313.x_1.x_3+0.0039.x_1.x_4-0.0101.x_1.x_5+0.0046.x_1.x_6+0.0031.x_1.x_7-0.0031.x_2.x_3-0.0085.x_2.x_4-0.0031.x_2.x_5-0.0054.x_2.x_6+0.x_2.x_7+0.007.x_3.x_4+0.0007.x_3.x_5+0.0046.x_3.x_6+0.0085.x_3.x_7+0.0031.x_4.x_5+0.0093.x_4.x_6+0.0085.x_4.x_7+0.0007.x_5.x_6+0.0062.x_5.x_7+0.0117.x_6.x_7 \quad (2)$$

Information of the authors

Pawar Padmakar., PhD, professor, K. K. Wagh Institute of Engineering Education and Research
e-mail: pjpawar1@rediffmail.com

Amol Dalavi, PhD, assistant professor, Symbiosis Institute of Technology
e-mail: amol.dalavi@sitpune.edu.in

Thorve K. M., K. K. Wagh Institute of Engineering Education and Research